Distinct Biogenesis Mechanisms for the Water Channels MIWC and CHIP28 at the Endoplasmic Reticulum†

Lan-bo Shi,‡ W. R. Skach,§ Tonghui Ma,‡ and A. S. Verkman*,‡

Departments of Medicine and Physiology, Cardiovascular Research Institute, University of California, San Francisco, California 94143-0521, and Department of Molecular and Cellular Engineering, University of Pennsylvania, Philadelphia, Pennsylvania 19104

Received January 31, 1995; Revised Manuscript Received March 31, 1995⊗

ABSTRACT: MIWC is a 32 kDa mercurial-insensitive water channel [Hasegawa *et al.* (1994) *J. Biol. Chem. 269,* 5497−5500] expressed in kidney collecting duct, brain ependymal cells, airways, and other tissues. We showed recently that the homologous water channel CHIP28 spanned the endoplasmic reticulum (ER) membrane 4 times with N- and C-termini in the cytoplasm [Skach *et al.,* (1994) *J. Cell Biol. 125,* 803−815]. Hydropathy analysis of MIWC indicated up to eight hydrophobic regions (HRs) comprising potential membrane-spanning domains. To determine MIWC transmembrane topology at the ER, 10 cDNA chimeras were constructed which encoded increasing lengths of MIWC upstream from a reporter epitope (prolactin P-domain) at residues 13, 46, 73, 92, 120, 140, 164, 209, 276, and 297, corresponding to putative polar extramembrane loops in the MIWC sequence. The chimeras were translated cell-free (rabbit reticulocyte lysate + ER-derived microsomes) and in *Xenopus* oocytes. Peptide chains were labeled with [^{35}S]methionine and immunoprecipitated with a P-domain antibody. Transmembrane topology as determined by protease accessibility of the P-reporter indicated six membrane-spanning domains with N- and C-termini in the cytoplasm. The predicted topology was confirmed by demonstrating N-linked glycosylation at native residue N131 and an engineered consensus site at residue 197. Membrane integration of the nascent chain, as assayed by extractability at pH 11.5, occurred after synthesis of the first HR (residues 1−46). Translocation was terminated by a stop transfer sequence in the second HR (residues 32−73) as demonstrated by translation of the heterologous construct, [prolactin signal sequence]-[globin]-[HR2]-P. In contrast to these results for MIWC, CHIP28 spanned the ER membrane 4 times, became integrated after 4 HRs (residues 1−107), and required HRs 2−4 (residues 35−139) to terminate translocation. Thus, despite their conserved sequences and similar function, significant differences exist in the early biogenesis of water channels CHIP28 and MIWC.

Several members of the MIP26 protein family have been shown recently to function as water-selective channels (aquaporins) in mammals, including CHIP28[1] (Preston *et al.,* 1992; Van Hoek & Verkman, 1992; Zhang *et al.,* 1993), WCH-CD (AQP-2; Fushimi *et al.,* 1993), MIWC (Hasegawa *et al.,* 1994b), and possibly GLIP (Ma *et al.,* 1994; Ishibashi *et al.,* 1994). Water permeability of CHIP28 and WCH-CD is inhibited by $HgCl_2$, whereas MIWC is mercurial-insensitive. MIWC has 41% amino acid identity to CHIP28 after sequence alignment, and functions as a water channel in epithelial cells of kidney collecting duct, trachea, ciliary body, and colonic villi, as well as in ependymal cells lining brain ventricles (Ma *et al.,* 1994; Frigeri *et al.,* 1995). An unusual feature of MIWC transcript expression is the tissue-specific expression of a spliced mRNA which does not appear to be translated. The CHIP28 water channel is also expressed widely in epithelia and endothelia of tissues involved in vectorial fluid transport (Zhang *et al.,* 1993; Nielsen *et al.,* 1993a; Hasegawa *et al.,* 1993, 1994a); however, expression of CHIP28 and MIWC is exclusive. WCH-CD is expressed primarily in the apical membrane of principal cells in kidney collecting duct (Nielsen *et al.,* 1993b).

Although no information is available about the structure of MIWC, recent morphological, spectroscopic, and molecular studies provide preliminary structural information about the homologous water channel CHIP28. Freeze−fracture electron microscopy showed that CHIP28 forms tetramers in reconstituted proteoliposomes and cell plasma membranes (Verbavatz *et al.,* 1993). Tetramers of similar size were observed at 2 nm resolution by electron crystallography (Walz *et al.,* 1994), and an oblong shape for individual monomers was visualized in a projection map at 1.2 nm resolution (Mitra *et al.,* 1994). Individual monomers comprising tetramers have ~45% helical content as shown by circular dichroism and Fourier transform infrared spectroscopy (Van Hoek *et al.,* 1993), and function independently as demonstrated by water permeability measurements on wild type-mutant heterodimers (Shi *et al.,* 1994). Two studies have addressed CHIP28 transmembrane topology. Skach *et al.* (1994) studied early biogenesis of CHIP28 at the endoplasmic reticulum (ER) using protein chimeras, native

† This work was supported by NIH Grants DK35124, HL42368, and HL51854.

* Address correspondence to this author at the Cardiovascular Research Institute, 1246 Health Sciences East Tower, University of California, San Francisco, CA 94143-0521. Phone: (415)-476-8530. Fax: (415)-665-3847.

‡ University of California, San Francisco.

§ University of Pennsylvania.

⊗ Abstract published in *Advance ACS Abstracts,* June 15, 1995.

[1] Abbreviations: MIWC, mercurial-insensitive water channel; CHIP28, channel forming integral protein of 28 kDa; WCH-CD, water channel-collecting duct; AQP, aquaporin; GLIP, glycerol intrinsic protein; AcAsn-Tyr-Thr, tripeptide inhibitor of N-linked glycosylation; ER, endoplasmic reticulum; RRL, rabbit reticulocyte lysate; XO, *Xenopus* oocyte.

0006-2960/95/0434-8250$09.00/0

truncated proteins, and a reporter of translocation. Analysis of cell-free and *Xenopus* oocyte translation products demonstrated that in the ER CHIP28 contained four membrane-spanning domains with N- and C-termini in the cytoplasm. Preston *et al.* (1994) studied a presumably matured form of full-length CHIP28 containing internal epitope tags. They also found a cytoplasmic location for the N- and C-termini, but concluded that there were six membrane-spanning domains. Several factors might account for differences in the detailed topological assignment (see Discussion), including the presence of multiple topological isoforms of CHIP28 early in its biogenesis or sequential folding and maturation of CHIP28 after initial ER synthesis.

Because of their closely related function and sequence homology, we sought to determine whether MIWC, like CHIP28, also utilized an unconventional mechanism of biogenesis. Therefore, the strategy employed to study CHIP28 was applied to determine the mechanism of MIWC biogenesis at the ER membrane. Unexpectedly, the biogenesis of MIWC was quite different from that of CHIP28. Analysis of the protease sensitivity of a reporter epitope fused to 10 sequential sites in MIWC defined 6 membrane-spanning segments. The deduced topology was confirmed by demonstrating N-linked glycosylation at a native and an engineered site in extramembrane loops predicted to reside in the ER lumen. Further, analysis of biogenesis indicated that unlike CHIP28, membrane integration of MIWC occurred after synthesis of one hydrophobic region (46 amino acids), and that chain translocation into the ER lumen was arrested by a stop transfer sequence encoded within the second hydrophobic region (amino acids 32−73). Thus, MIWC biogenesis in the ER sharply contrasted with CHIP28 in both the experimentally-deduced transmembrane topology and the mechanism of biogenesis.

MATERIALS AND METHODS

cDNA Constructs. Plasmid pSP64T-MIWC (Hasegawa *et al.*, 1994b) was used as template for the PCR amplifications below. Clones 1−10 were generated using the sense oligonucleotide 5′-AGGATCTCGGCTAGCGATGACC-3′ to bp 2757 of plasmid SP64 (Promega) and a series of 10 antisense oligonucleotides to regions of the MIWC coding sequence, which introduced a *Bst*EII restriction site at codons 13, 46, 73, 92, 120, 140, 164, 209, 276, and 297. Antisense oligonucleotides: (1) GACCGCGGTCACCAAGGCTTGAGTCCAGAC; (2) GAGGACGGTCACCACAGGTAGGGGGTTC; (3) CGCTGGGGTCACCTGGCCACCGCTGATGTG; (4) GTAGAAGGTCACCTTGGCGATGCTGATC; (5) CAATCCGGTCACCACGCTGGGGGG; (6) GATTATGGTCACCACCAGGAGCCCATG; (7) AGCAACGGTCACCGTAACATCAGTCCGTTTG; (8) AACCCAGGTCACCCAGTGGTTTTCCCAG; (9) CACATGGGTCACCCCGGGCTTCAGG; (10) AGAAGAGGTCACCTCTCCAGACGAGTC. After 20 cycles of PCR, fragments were digested with *Nhe*I and *Bst*EII, gel-purified, and ligated into *Nhe*I/*Bst*EII-digested vector S.L.ST.gG.P, in which P represents the COOH-terminal 142 residues from bovine prolactin (Skach *et al.*, 1993). These "MIWC-P" chimeric clones thus encode a translation initiation Met at codon 1 and varying lengths of MIWC followed by the P reporter. All constructs were confirmed by sequence analysis.

Clone S.gG.X.P encodes an NH_2-terminal signal sequence derived from preprolactin (S), a chimpanzee α-globin domain containing an engineered N-linked glycosylation site (gG), an internal fragment of MIWC (X = residues 32−73, 32−92, or 32−120), and the P reporter (Skach *et al.*, 1994). The X MIWC fragment was generated by PCR using the sense oligonucleotide 5′-AGCGTGGTGACCACCATTAACTGGGG-3′ and antisense oligonucleotides 3, 4, or 5. After 20 cycles of PCR using pSP64T-MIWC as template, the amplified fragment was digested with *Bst*EII, gel-purified, and ligated into vector S.gG.TM2.P, from which the TM2 sequence was removed (Skach *et al.*, 1994; Rothman *et al.*, 1988) at the *Bst*EII site between the gG and P-domains.

MIWC mutant GPA[197−199]NGT was generated using the *in vitro* mutagenesis system (Promega). The MIWC coding sequence, together with an upstream *Xenopus* globin enhancer sequence, was subcloned into plasmid pAlter1 at *Hin*dIII and *Eco*RI restriction sites. Oligonucleotide 5′-GTTTTCCCAGTTTCCCATGATAAC*GGTAC*-*CGTT*AAAGGATCGAGCTGGATTCATGCTG-3′ contains six changes, G→A, G→A, C→G, C→G, G→A, and A→C at bp 589, 590, 592, 593, 595, and 597, giving three codon changes, Gly→Asn, Pro→Gly, and Ala→Thr at residues 197, 198, and 199, and creating a *Kpn*I restriction site.

Cell-Free and Oocyte Translation. cRNA was transcribed with SP6 polymerase using 2 mg of plasmid DNA in a 10 mL volume at 40 °C for 1 h (Skach *et al.*, 1994). For cell-free translation, the transcription mixture was added to rabbit reticulocyte lysate containing [^{35}S]methionine for 1 h at 24 °C. Microsomal membranes from dog pancreas were added to a final concentration of 8 OD_{280}. In some experiments, a tripeptide inhibitor of oligosaccharyltransferase, AcAsn-Tyr-Thr, was added at a final concentration of 0.2 mM. For expression in *Xenopus* oocytes, 50 nL of the transcription mixture + [^{35}S]methionine was injected into stage VI oocytes. After a 2 h incubation at 18 °C, oocytes were homogenized on ice in 0.25 M sucrose, 50 mM KAc, 5 mM $MgAc_2$, 1 mM DTT, and 50 mM Tris (pH 7.5). For proteolysis, $CaCl_2$ (10 mM) and proteinase K (PK) were added to the reticulocyte lysate or oocyte homogenate in the absence or presence of 1% Triton X-100 and incubated for 1 h on ice (Skach *et al.*, 1993). Protease activity was quenched by PMSF (10 mM) and boiling in 1% SDS, 0.1 M Tris (pH 8). Reticulocyte lysate samples were analyzed directly by SDS−PAGE; oocyte samples were centrifuged (14000*g*, 15 min), and supernatants were used for immunoprecipitation.

Membrane integration was assessed by protein extraction at high pH. Oocyte homogenates were diluted 1000-fold in either sodium carbonate (0.1 M, pH 11.5) or neutral buffer (0.25 M sucrose, 0.1 M Tris, pH 7). Samples were incubated on ice for 30 min and centrifuged at 150000*g* for 30 min. Protein from supernatants was precipitated in 20% trichloroacetic acid, washed in acetone, and dissolved in 1% SDS, 0.1 M Tris (pH 8) prior to immunoprecipitation.

Immunoprecipitation and Autoradiography. A rabbit polyclonal anti-prolactin antibody (U.S. Biochemical Corp., 1:1000) or an anti-globin antibody was added to translation products in 0.1 M NaCl, 1% Triton X-100, 2 mM EDTA, 0.1 mM PMSF, and 0.1 M Tris (pH 8). After 15 min, protein A Affigel (BioRad) was added for 6−10 h at 4 °C. Samples were washed 3 times in 0.1 M NaCl, 1% Triton X-100, 2 mM EDTA, and 0.1 M Tris (pH 8) and twice in 0.1 M NaCl, 0.1 M Tris (pH 8), resolved by SDS−PAGE, and autoradiographed.

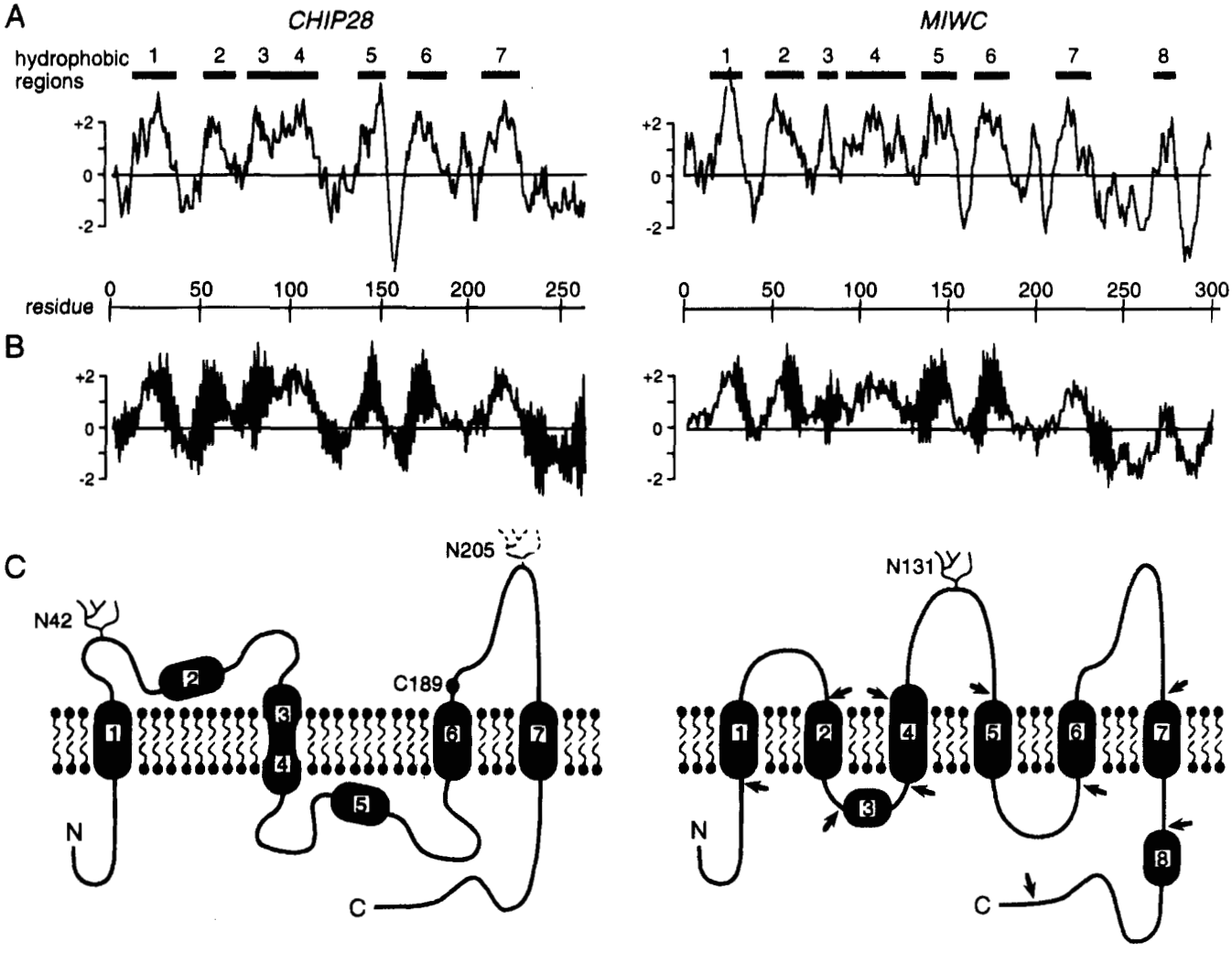

FIGURE 1: Water channel hydropathy profiles and topology. (A) Kyte−Doolittle hydropathy profiles for CHIP28 and MIWC (window width 7), showing distinct hydrophobic regions (HRs). (B) Amphiphilicity profiles (periodicity 3.6, window width 19) generated as described by Van Hoek *et al.* (1993); amphiphilic α-helix is suggested by high-amplitude oscillation in hydrophobic regions. (C) Left: Deduced ER topology for CHIP28 (Skach *et al.*, 1994) showing four membrane-spanning domains, N-linked glycosylation at native residues N42 and (under some conditions) N205, and the $HgCl_2$ binding site at residue C189. HRs are labeled as in (A). The region above the membrane corresponds to the ER lumen. Right: Proposed ER topology for MIWC showing 6 membrane-spanning domains, native N-linked glycosylation site N131, and fusion sites for the 10 MIWC-P chimeras (arrows). See text for details.

RESULTS

Figure 1 compares Kyte−Doolittle hydropathy profiles [conventional hydrophobicity (A) and α-helix amphiphilicity (B); see Van Hoek *et al.* (1993)] for CHIP28 and MIWC. Hydrophobic regions (HRs) as predicted by the hydrophobicity profile are indicated by the bars at the top of the figure. Seven HRs were defined previously for CHIP28, four of which were shown to span the ER membrane (panel C, left; Skach *et al.*, 1994). On the basis of the sequence alignment of CHIP28 and MIWC (Hasegawa et al., 1994), eight HRs are indicated for MIWC, the first seven of which correspond to HRs in CHIP28. Six of the HRs in MIWC (HRs 1, 2, 4−7) might form transmembrane helical domains based on their length, and four of the HRs (HRs 1, 2, 5, 6) might form amphipathic helices based on the amphiphilicity profile; a proposed ER topology for MIWC is shown in Figure 1C, right. The single native consensus site for N-linked glycosylation (N131) of MIWC is indicated. The fusion sites in the MIWC-P chimeras (referred to as "clone 1", ..., "clone 10") are shown by arrows, and correspond to residues in putative extramembrane domains. It is noted that although MIWC and CHIP28 share a number of amino acid motifs conserved in MIP family members (Wistow *et al.*, 1991), their modest amino acid sequence identity (41%) and their different sizes and hydropathy profiles do not rule out distinct transmembrane topologies and/or biogenesis mechanisms.

Figure 2 shows an autoradiogram of total [^{35}S]methionine-labeled translation products from cell-free translation of the MIWC-P clones 1−10 in rabbit reticulocyte lysate in the absence and presence of dog pancreatic microsomes. The clones were translated efficiently, and the protein products had the expected sizes. In the presence of microsomes, clone 2 generated an additional translation product of ~14 kDa, probably resulting from exposure of a cryptic cleavage site for signal peptidase near HR1. Similar unmasking of cryptic cleavage sites has been reported for CHIP28 and other transmembrane proteins (Skach *et al.*, 1994; Skach & Lingappa, 1993; Nothwehr & Gordon, 1989). Translation products from clone 6 in the presence of microsomes contained a second band at greater molecular size which disappeared when AcAsn-Tyr-Thr was included in the translation mixture (not shown), indicating N-linked glycosylation at residue N131. N-Linked glycosylation was not observed in the other clones. These results are consistent

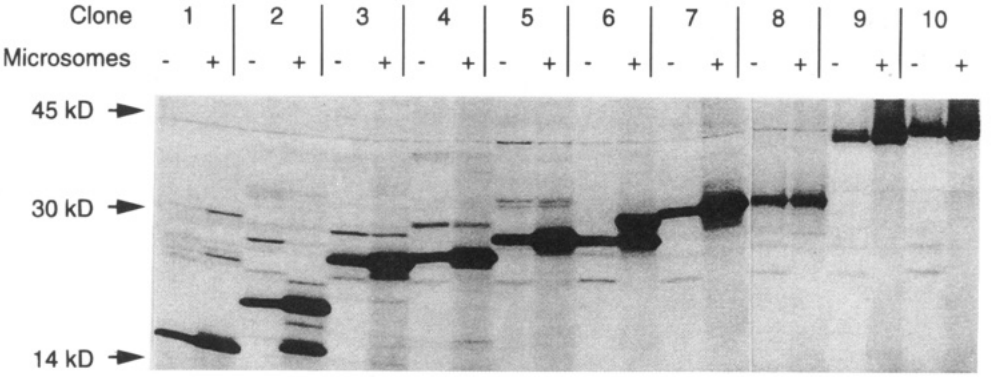

FIGURE 2: Autoradiogram of total cell-free translation products of MIWC-P chimeric clones containing the prolactin P-domain downstream from truncated fragments of MIWC (see Materials and Methods). Chimeric clones 1−10 were translated in rabbit reticulocyte lysate in the presence of [^{35}S]methionine and in the absence or presence of pancreatic microsomes as indicated.

with immunoblot analysis showing that full-length MIWC is not glycosylated in native kidney membranes (Frigeri *et al.*, 1995).

To determine ER transmembrane topology, MIWC-P clones 1−10 were expressed in *Xenopus* oocytes, and translation products from oocyte membranes were either immunoprecipitated with anti-prolactin antisera directly or treated with proteinase K prior to immunoprecipitation (Figure 3).[2] For each clone, the first two lanes show cell-free translation products without and with pancreatic microsomes; the last three lanes show immunoprecipitated oocyte translation products prior to and following proteinase K digestion in the absence and presence of Triton X-100. The deduced topology for each clone is shown at the bottom of the figure. Protection of the prolactin P-domain from digestion by proteinase K, as deduced from the similar band intensities in the third and fourth lanes for each clone, indicates that the prolactin P-domain resides in the ER lumen. When expressed in oocytes, reporter domains generated from clones 1, 3, 4, 7, 9, and 10 were proteinase K-sensitive, whereas clones 2, 6, and 8 generated chains with protected P-domain. Note that the action of proteinase K on exposed extralumenal loops in the cytosol caused an ~5 kDa decrease in the apparent size of the protected bands in clones 6 and 8, most likely due to proteinase K digestion of the first cytosolic loop between HR2 and HR4. Clone 5 was relatively insensitive to proteinase K; however, the autoradiogram cannot be interpreted unambiguously (lane 24), probably because the fusion site was located at or near a membrane-spanning domain. Cell-free and oocyte translation products for clone 2 showed protected bands resulting from signal peptidase cleavage as discussed above (upward arrow, lane 7). Only clone 6 showed N-linked glycosylation (downward arrow, lane 27) as demonstrated by the upper band at ~3 kDa above the lower band, and the disappearance of the upper band when the tripeptide inhibitor of N-linked glycosylation was present (not shown). The data suggest that in contrast to CHIP28, MIWC spans the ER membrane 6 times. The experiments in Figure 3 were conducted at 2 h after translation for interpretation of results in terms of ER topology (Skach *et al.*, 1994); this ER topology for MIWC remained unchanged over time in similar protease protection experiments carried out in oocytes pulsed with [^{35}S]methionine for 15 min and chased with excess nonradioactive methionine for 48 h (not shown).

There are three testable predictions of the six membrane-spanning model for MIWC topology, the first of which concerns membrane integration, as assessed by protein extractability at a high pH of 11.5 (Fujiki *et al.*, 1982). The MIWC-reporter clones were translated in the presence of [^{35}S]methionine, microsomes were incubated at pH 7.0 or 11.5 for 1 h, and supernatants (S) and pellets (P) were prepared by centrifugation. Figure 4 shows that a secretory control protein (full-length prolactin) was extracted into the supernatant at pH 11.5. Chains translated from clone 1 were extracted into the supernatant at pH 11.5 (downward arrow, lane 3) as expected. Chains translated from clones 3 and 4 appeared quantitatively in the pellet (downward arrows, lanes 12 and 16) at high pH. For clone 2, bands corresponding to the full-length (uncleaved) and cleaved peptides were seen. As expected, cleaved chains (see also Figure 2, lane 9) were not integrated into the ER membrane (upward arrow, lane 7). In contrast, the full-length translation product from clone 2 was integrated into the membrane as shown by the downward arrow in lane 8. The full-length translation product from clone 2, containing only 46 amino acids and a single membrane-spanning segment, HR1, was completely integrated into the ER membrane. As reported previously, membrane integration of CHIP28 occurred after the fourth HR, corresponding to synthesis of 107 amino acids (Skach *et al.*, 1994).

The topology model next predicts that residues ~32−46, 126−140, and 184−209 reside in extramembrane loops located in the ER lumen (see Figure 1C, right). Because N-linked glycosylation reactions occur only in the ER lumen, we examined the glycosylation pattern of MIWC after engineering consensus glycosylation sites in the first and thirds putative lumenal loops. The glycosylation of native residue N131 in clone 6 (Figure 3, lanes 27, 28) indicated a lumenal location for the second loop. It is noted that no glycosylation occurred in clones 7−10 (Figure 3) and in native kidney MIWC (Frigeri *et al.*, 1995). In general, consensus sites for N-linked glycosylation in polytopic proteins which reside in the ER lumen may be glycosylated efficiently, poorly, or not at all (Landbolt-Martincorene & Reithmeier, 1994). Statistical analysis of polytopic glycoproteins suggests that extracytosolic loops require a minimum

[2] It was demonstrated previously that both full-length and spliced mRNAs encoding MIWC are expressed in a tissue-specific manner (Hasegawa *et al.*, 1994b), where 165 nucleotides (corresponding to residues 127−182) are missing in the spliced message. We attempted to study the topology of proteins translated from the spliced form of MIWC in three additional chimeric clones constructed by PCR using the spliced MIWC cDNA as template, 5′-sense primer, and antisense primers 8, 9, and 10. However, all three cDNAs were unsuitable for analysis of topology because they were translated inefficiently in both cell-free and oocyte systems.

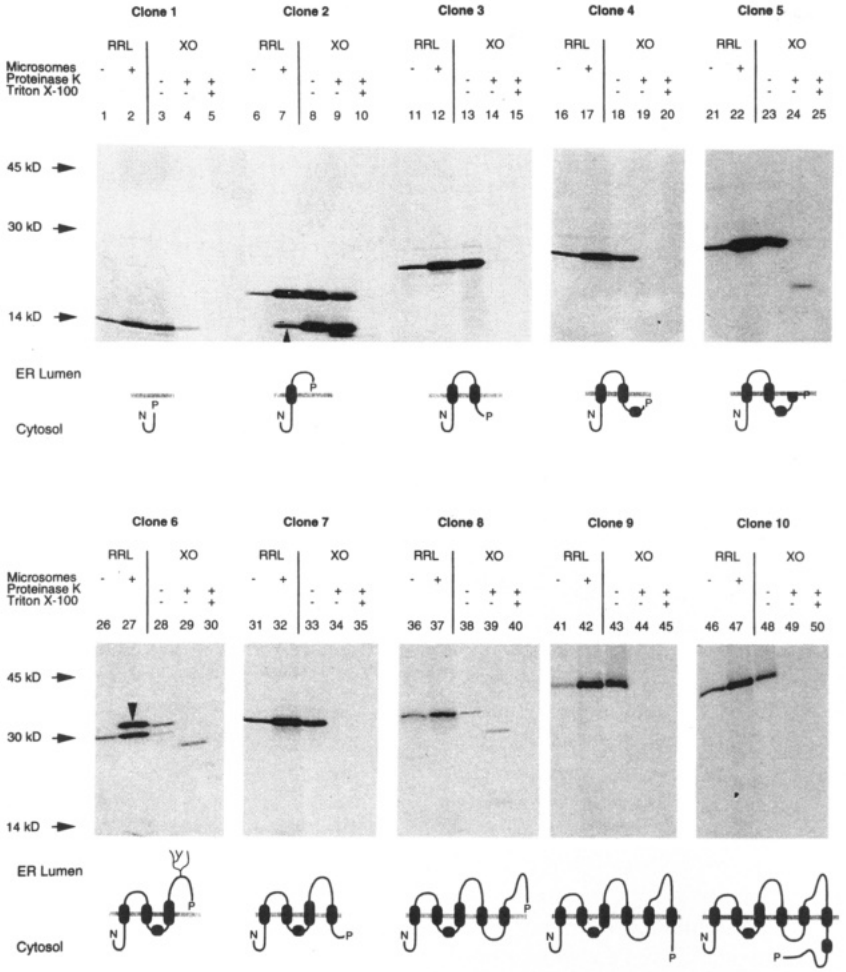

FIGURE 3: Topology of MIWC at the ER deduced from protease sensitivities of MIWC-P chimeric clones 1−10 translated in *Xenopus* oocytes. Clones were translated cell-free or in oocytes, immunoprecipitated by anti-prolactin antisera, and subject to SDS−PAGE and autoradiography (see Materials and Methods). For each clone, translation was carried out in rabbit reticulocyte lysate in the absence or presence of microsomes (first two lanes) and in *Xenopus* oocytes without proteinase K treatment and with proteinase K in the absence or presence of Triton X-100 (last three lanes). The upward arrow in lane 7 corresponds to a peptidase-cleaved translated product from clone 2 (see text). The downward arrow in lane 27 corresponds to an N-linked glycosylated form of the molecule (at residue N131). The topology deduced from the proteolysis results is shown at the bottom of the gels for each clone.

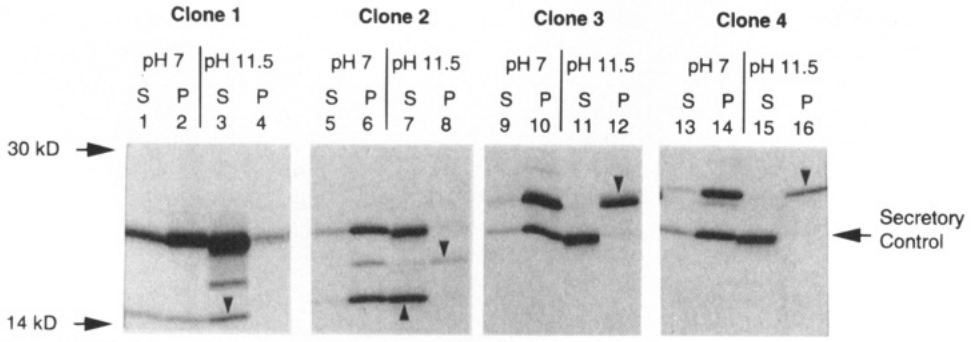

FIGURE 4: Integration of MIWC determined by extraction at high pH. MIWC-P clones 1−4 and a secretory control protein (full-length prolactin) were translated cell-free in the presence of [^{35}S]methionine and canine ER-derived microsomes. Microsomes were incubated at pH 7 or 11.5 as described under Materials and Methods, and centrifuged to give supernatants (S) and pellets (P). Downward arrows correspond to recovery of full-length translation products for each clone. The upward arrow in lane 7 corresponds to the high-pH extraction of a peptidase-cleaved form of clone 2.

of ~30 amino acids for efficient glycosylation. The extracellular loop containing residue N131 has only ~26 amino acids. It is likely that the additional amino acids of the reporter domain in clone 6 facilitate glycosylation at N131. Similar observations have been made for N-linked glycosylation of CHIP28 (Skach *et al.*, 1994) and rhodopsin (Nathans & Hogness, 1983).

N-Linked glycosylation was examined in MIWC mutants in which glycosylation consensus sites were engineered in the first and third extramembrane loops predicted to reside in the ER lumen. Figure 5A shows total cell-free translation products for MIWC mutant GPA[197−199]NGT. This mutant was partially glycosylated, confirming a lumenal location for the third lumenal loop. Similar experiments were carried out for MIWC mutant GG[38−39]NA, which contains an N-linked glycosylation site in the first lumenal loop; however, <10% of translated chains were glycosylated (not shown). Because of the variable efficiency of N-linked

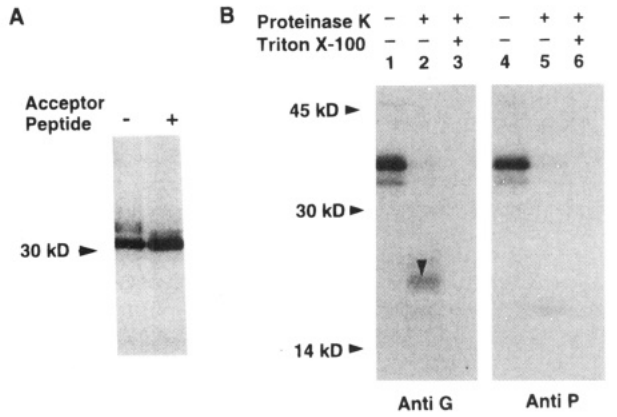

FIGURE 5: (A) N-Linked glycosylation of the engineered consensus site at residue 197. Cell-free translation of MIWC mutant GPA-[197−199]NGT, which contains a consensus site for N-linked glycosylation in the third extramembrane lumenal loop. Where indicated, the tripeptide inhibitor of N-linked glycosylation was present during translation. (B) Analysis of stop transfer activity encoded by the MIWC amino acid sequence. Chimeric clone S.gG-[32−92]-P (see Materials and Methods) was translated cell-free in the presence of [^{35}S]methionine and canine ER-derived microsomes. Microsomes were treated without or with proteinase K in the absence or presence of detergent as indicated. Translated products were immunoprecipitated with P-domain or G-domain antibody. The downward arrow in lane 2 indicates a truncated MIWC fragment with a protected G-domain.

glycosylation, a negative result for mutant GG[38−39]NA is noninformative.

The third model prediction concerns insertion of the first and second hydrophobic regions of MIWC. In CHIP28, the amino acids encoded by HRs 2−4 (amino acids 35−139) had intrinsic stop transfer activity when expressed in the chimeric cassette S.gG-X-P (see Materials and Methods), whereas the second and third HRs failed to stop translocation (Skach *et al.*, 1994). Because the second (rather than the fourth) hydrophobic region of MIWC completes the first transmembrane loop at the ER, it was predicted that HR2 of MIWC should by itself possess stop transfer activity. Figure 5B shows cell-free translation of S.gG-X-P, where X encoded MIWC residues 32−92. If fragment X has intrinsic stop transfer activity, then the translated chimeric protein would be directed into a type 1 membrane topology with the G-domain in the ER lumen and the P-domain in the cytosol. Thus, the P-domain would be digested by proteinase K, leaving a smaller peptide fragment with intact G-domain. Alternatively, if X lacked stop transfer activity, chains would be translocated into the ER lumen and remain fully protected from protease digestion. Figure 5B shows that the P-domain was digested (lane 5), as assessed by P-domain immunoprecipitation, and the remaining G-domain was intact but contained within a truncated protein fragment (arrow, lane 2), as shown by G-domain immunoprecipitation. Therefore, residues 32−92 have intrinsic stop transfer activity. Similar results were observed when X corresponded to residues 32−73 and 32−120 (not shown), indicating that the stop transfer activity of HR2 was not sensitive to the precise length of the downstream sequence. These results indicate that unlike CHIP28, the second HR of MIWC terminates translocation and spans the ER membrane, supporting the data in Figures 3 and 4 that MIWC and CHIP have different transmembrane topologies and mechanisms of biogenesis at the ER.

DISCUSSION

The data indicate that although the MIWC and CHIP28 water channels belong to the same family of small hydrophobic channel-forming proteins (Wistow *et al.*, 1991), there are significant differences in their mechanisms of biogenesis and transmembrane topologies at the endoplasmic reticulum. Previous tissue localization studies showed that MIWC and CHIP28 were widely distributed in plasma membranes of cells involved in fluid transport (Hasegawa *et al.*, 1993, 1994a,b; Nielsen *et al.*, 1993a; Bondy *et al.*, 1993; Folkesson *et al.*, 1994); however, MIWC and CHIP28 did not colocalize in the same cells. Other differences include transcript expression, where both a full-length form and a spliced form of MIWC are expressed, but only full-length CHIP28 is expressed, and biochemical properties, such as solubilization of MIWC but not CHIP28 by the anionic detergent *N*-lauroylsarcosine. Although MIWC and CHIP28 appear to function exclusively as selective water-transporting proteins, other members of the MIP26 family have different functions, such as transport of glycerol (Ma *et al.*, 1994; Sweet *et al.*, 1990) and ions or other small solutes (Zampighi *et al.*, 1989). Therefore, because of differences in the expression and function of MIP26 family members, as well as in the predicted secondary structure based on hydropathy profiles (Verkman, 1993), individualized analysis of structure and function is warranted for each protein in the MIP26 family.

The deduced transmembrane topology of MIWC at the ER reported here differed from that determined previously for CHIP28 (Skach *et al.*, 1994); MIWC contained six membrane-spanning domains, whereas CHIP26 contained only four. The principal difference in topology was in the first half of the molecule—hydrophobic region 2 formed the second membrane-spanning domain in MIWC, whereas hydrophobic regions 2, 3, and 4 were required to complete the second membrane-spanning domain in CHIP28. This conclusion was corroborated by analysis of the intrinsic stop transfer activity of various MIWC fragments, and of the minimum MIWC fragment required to achieve membrane integration. When translated in a defined chimeric cassette, HR2-MIWC had intrinsic stop transfer activity, whereas HR2-CHIP28 and HR2−3-CHIP did not. Membrane integration occurred after HR1 (46 amino acids) in MIWC, but after HR4 (107 amino acids) in CHIP28. Finally, analysis of native and engineered N-linked glycosylation sites supported the topology for MIWC deduced from proteolysis studies.

It should be noted that the current study analyzes the topology of MIWC at the ER, and not subsequent modification or targeting events involved in insertion into the plasma membrane. Recent studies suggest that the topology for CHIP28 early after biogenesis at the ER membrane may differ from that in the plasma membrane. Ma *et al.* (1993) reported that ER membranes from fractionated CHO cells transfected with CHIP28 were not water-permeable, whereas Golgi and surface membrane vesicles were highly water-permeable. Skach *et al.* (1994) examined the transmembrane topology of CHIP28 in oocytes by engineering a reporter of translocation into nine sequential sites in the CHIP28 coding region and by cell-free translation of truncated CHIP28 cDNAs. It was concluded from both cell-free and oocyte data that CHIP28 spanned the membrane 4 times with the N- and C-termini in the cytoplasm. Independent support for this model was provided by identifying and characterizing

signal sequences which initiate chain translocation into the ER lumen and stop transfer sequences which terminate translocation. It was proposed that the first signal sequence of CHIP28 (residues 1−52) targets the nascent chain−ribosome complex to the ER membrane, initiates chain translocation, and spans the membrane with its NH_2-terminus in the cytosol (C-trans or type 1 topology). Translocation is subsequently terminated by a stop transfer sequence within HR4 (possibly together with HR3) which forms the second membrane-spanning helix. A second internal signal sequence (residues 155−186) reinitiates translocation and forms the third membrane-spanning helix. Stop transfer activity of HR7 terminates translocation and establishes the fourth and final membrane-spanning helix.

Preston *et al.* (1994) mapped CHIP28 topology in *Xenopus* oocytes by inserting epitopes into full-length CHIP28 cDNA. Several of the chimeric proteins were functional in water transport. Of the functional chimeras, the protease accessibility of epitope tags expressed at the cell surface of intact oocytes confirmed that peptide regions between HRs 1 and 2 and between HRs 6 and 7 reside outside the cytosol, in agreement with the topology at the ER. However, the peptide region beyond HR4 was also extracytosolic in some chains (glycosylated chains), contrasting with the ER topology in which the region following HR4 resided in the cytosol. On the basis of these results, as well as the protease accessibility of CHIP28 chimeras in intracellular vesicles, Preston *et al.* proposed that CHIP28 spanned the membrane 6 times. Differences in CHIP28 topology predicted by these two studies might be due to a number of factors. It is possible that the reporters or restriction sites used to generate chimeras introduce artifactual changes in the observed topology. CHIP28 biogenesis may exhibit an unexpected level of regulation. CHIP28 topology at the ER membrane might be modified by subsequent steps of functional maturation. Alternately, multiple isoforms of CHIP28 may be generated for a single cDNA sequence, perhaps with different stabilities and/or efficiencies for trafficking to the cell surface.

Recent experiments utilizing an engineered multispanning protein in *Escherichia coli* provided evidence that multiple protein isoforms may be generated under certain conditions (Gafvelin & Von Heijne, 1994). By adjusting the charges on connecting loops, proteins were engineered in which one or more hydrophobic regions were "left out" and did not span the membrane, as has been proposed for HRs 2 and 5 in CHIP28 (Skach *et al.*, 1994). Other engineered constructs generated proteins which exhibited more than one topological isoform. Recent studies of CHIP28 by pulse−chase methods support the conclusion that the apparent topology of CHIP28 early in its biogenesis at the ER membrane is different from that found at later times (Skach & Verkman, 1995). In contrast to the complex and interesting mechanisms emerging for CHIP28 biogenesis, we conclude here that only one stable MIWC isoform is generated at the ER with a transmembrane topology consisting of six membrane-spanning segments.

ACKNOWLEDGMENT

We thank Dr. V. Lingappa for helpful advice and critical review of the manuscript.

REFERENCES

Bondy, C., Chin, E., Smith, B. L., Preston, G. M., & Agre, P. (1993) *Proc. Natl. Acad. Sci. U.S.A. 90*, 4500−4504.

Folkesson, H. G., Matthay, M. A., Hasegawa, H., Kheradmand, F., & Verkman, A. S. (1994) *Proc. Natl. Acad. Sci. U.S.A. 91*, 4970−4974.

Frigeri, A., Gropper, M. A., Turck, C. W., & Verkman, A. S. (1995) *Proc. Natl. Acad. Sci. U.S.A. 92*, 4328−4331.

Fujiki, Y. A., Hubbard, A. L., Fowler, S., & Lazarow, P. B. (1982) *J. Cell Biol. 93*, 97−102.

Fushimi, K., Uchida, S., Hara, Y., Hirata, Y., Marumo, F., & Sasaki, S. (1993) *Nature 361*, 549−552.

Gafvelin, G., & Von Heijne, G. (1994) *Cell 77*, 401−412.

Hasegawa, H., Zhang, R., Dohrman, A., & Verkman, A. S. (1993) *Am. J. Physiol. 264*, C237−C245.

Hasegawa, H., Lian, S. C., Finkbeiner, W. E., & Verkman, A. S. (1994a) *Am. J. Physiol. 266*, C893−903.

Hasegawa, H., Ma, T., Skach, W., Matthay, M. M., & Verkman, A. S. (1994b) *J. Biol. Chem. 269*, 5497−5500.

Ishibashi, K., Sasaki, S., Fushimi, K., Uchida, S., Kuwahara, M., Saito, H., Furukawa, T., Nakajima, K., Yamaguchi, Y., Gojobori, T., & Marumo, F. (1994) *Proc. Natl. Acad. Sci. U.S.A. 91*, 6269−6273.

Landolt-Marticorena, C., & Reithmeier, R. (1994) *Biochem. J. 302*, 253−260.

Ma, T., Frigeri, A., Tsai, S.-T., Verbavatz, J. M., & Verkman, A. S. (1993) *J. Biol. Chem. 268*, 22756−22764.

Ma, T., Frigeri, A., Hasegawa, H., & Verkman, A. S. (1994) *J. Biol. Chem. 269*, 21845−21849.

Mitra, A. K., Yaeger, M., Van Hoek, A. N., Wiener, M. C., & Verkman, A. S. (1994) *Biochemistry 33*, 12735−12740.

Nathans, J., & Hogness, D. S. (1983) *Cell 34*, 807−814.

Nielsen, S., Smith, B. L., Christensen, E. I., Knepper, M. A., & Agre, P. (1993a) *J. Cell Biol. 120*, 371−383.

Nielsen, S., DiGiovanni, S. R., Christensen, E. I., Knepper, M. A., & Harris, H. W. (1993b) *Proc. Natl. Acad. Sci. U.S.A. 90*, 11663−11667.

Nothwehr, S. F., & Gordon, J. I. (1989) *J. Biol. Chem. 264*, 3979−3987.

Preston, B. M., Carroll, T. P., Guggino, W. B., & Agre, P. (1992) *Science 256*, 385−387.

Preston, G. M., Jung, J. S., Guggino, W. B., & Agre, P. (1994) *J. Biol. Chem. 269*, 1668−1673.

Rothman, R. E., Andrews, D. W., Calayag, M. C., & Lingappa, V. R. (1988) *J. Biol. Chem. 263*, 10470−10480.

Shi, L.-B., Skach, W., & Verkman, A. S. (1994) *J. Biol. Chem. 269*, 10417−10422.

Skach, W. R., & Lingappa, V. (1993) in *Mechanisms of Intracellular Trafficking and Processing of Preproteins* (Loh, Y. P., Ed.) CRC Press, Ann Arbor, MI.

Skach, W., & Verkman, A. S. (1995) *Biophys. J. 68*, A344 (Abstr.).

Skach, W. R., Calayag, M. C., & Lingappa, V. R. (1993) *J. Biol. Chem. 268*, 6903−6908.

Skach, W., Shi, L.-B., Calayag, M. C., Frigeri, A., Lingappa, V. R., & Verkman, A. S. (1994) *J. Cell Biol. 125*, 803−815.

Sweet, G., Gandor, C., Voegele, R., Wittekindt, N., Beuerle, J., Truniger, V., Lin, E. C. C., & Boos, W. (1990) *J. Bacteriol. 172*, 424−430

Van Hoek, A. N., & Verkman, A. S. (1992) *J. Biol. Chem. 267*, 18267−18269.

Van Hoek, A. N., Wiener, M., Bicknese, S., Miercke, L., Biwersi, J., & Verkman, A. S. (1993) *Biochemistry 32*, 11847−11856.

Verbavatz, J. M., Brown, D., Sabolic, I., Valenti, G., Ausiello, D. A., Van Hoek, A. N., Ma, T., & Verkman, A. S. (1993) *J. Cell Biol. 123*, 605−618.

Verkman, A. S. (1993) *Water Channels*, R. G. Landes Co., Austin, TX.

Walz, T., Smith, B. L., Zeidel, M. L., Engel, A., & Agre, P. (1994) *J. Biol. Chem. 269*, 1583−1586.

Wistow, G. J., Pisano, M. M., & Chepelinski, A. B. (1991) *Trends Biochem. Sci. 16*, 170−171.

Zampighi, G. A., Hall, J. E., Ehring, G. R., & Simon, S. A. (1989) *J. Cell Biol. 108*, 2255−2275.

Zhang, R., Skach, W., Hasegawa, H., Van Hoek, A. N., & Verkman, A. S. (1993) *J. Cell Biol. 120*, 359−369.

BI950218B